CHEMISTRY
A EUROPEAN JOURNAL

DOI: 10.1002/chem.200701731

# Self-Assembled Structures in Organogels of Amphiphilic Diblock Codendrimers

**Miao Yang,[a] Zijian Zhang,[a] Fei Yuan,[a] Wei Wang,*[a] Sandra Hess,[b] Karen Lienkamp,[b] Ingo Lieberwirth,[b] and Gerhard Wegner*[b]**

**Abstract:** Amphiphilic diblock codendrimers consisting of dendrons of hydroxyl-containing poly(methallyl dichloride) (PMDC) and long alkyl-containing poly(urethane amide) (PUA) were synthesized in different generations. These codendrimers were found to self-assemble into ribbonlike aggregates in organic solvent and further formed three-dimensional networks and behaved macroscopically as gels. The width of the self-assembled ribbons decreases with the generation of both dendritic blocks. Multiple intermolecular hydrogen bonds between amide and hydroxyl groups were found to be the main driving force to form these self-assembled gels.

**Keywords:** amphiphiles · dendrimers · gels · molecular interactions · self-assembly

## Introduction

Over recent decades, there has been great interest in exploring novel gel-phase materials particularly because of their potential applications in cosmetics, food processing, drug delivery etc.[1] Normally, gelators form well-defined supramolecular structures on several hierarchical levels, first by molecular recognition followed by anisotropic aggregation in one or two dimensions and finally, three-dimensional networks form that can trap solvents.[1] Therefore, investigations in this field, particularly in exploring novel gelators, can fully express the bottom-up concept from designing and then synthesizing novel gelator molecules to constructing supramolecular structures mainly through self-assembly.

Dendrimer-based molecules acting as promising candidates have attracted great attention in supramolecular self-assembly owing to their well-defined architectures and diversity in functionalization.[2] It has been demonstrated that modified dendrons can act as building blocks to induce the formation of spherical or cylindrical supramolecular objects.[3] It is interesting to mention that bolaform dendritic molecules with amphiphilic features assemble in their gel phase into one-dimensional aggregates, which further develop into cross-linked networks in organic or aqueous media.[4,5] Meanwhile, nanoribbonlike supramolecular structures have also been found in gels of dendronized rod–coil molecules.[6] These works have provided a first indication that the molecular architecture may be one of the key factors in the gel formation of dendritic molecules.[7] To design novel gelators, however, we still need to clarify the importance of some molecular parameters, such as shape, polarity, and intermolecular interaction, on the formation of supramolecular structures in their gels.

Recently our group has concentrated our efforts on the self-assembly of diblock codendrimers.[8] They have previously been shown to provide versatile supramolecular shapes and architectures when tuning their shape and polarity. In this work we study the effects of molecular architecture, multiple interactions, and the polarity of the block codendrimers on their self-assembly characteristics during gel formation in organic media. To achieve this goal, a series of amphiphilic diblock codendrimers was prepared, as shown in Scheme 1. They contain amide branches for the formation of multiple hydrogen bonds, hydroxyl groups for hydrophilic ends, and alkyl chain tails for stabilization of the aggregates through hydrophobic interactions. Clearly, changing the gen-

[a] M. Yang, Z. Zhang, Dr. F. Yuan, Prof. Dr. W. Wang
The Key Laboratory of Functional Polymer Materials of the Ministry of Education
Institute of Polymer Chemistry, College of Chemistry
Nankai University, Tianjin 300071 (China)
Fax: (+86) 22-234-98126
E-mail: weiwang@nankai.edu.cn

[b] Dr. S. Hess, Dr. K. Lienkamp, Dr. I. Lieberwirth, Prof. Dr. G. Wegner
Max-Planck-Institute for Polymer Research
Ackermannweg 10, 55128, Mainz (Germany)
Fax: (+49) 6131-379-330
E-mail: wegner@mpip-mainz.mpg.de

Supporting information for this article is available on the WWW under http://www.chemeurj.org/ or from the author.

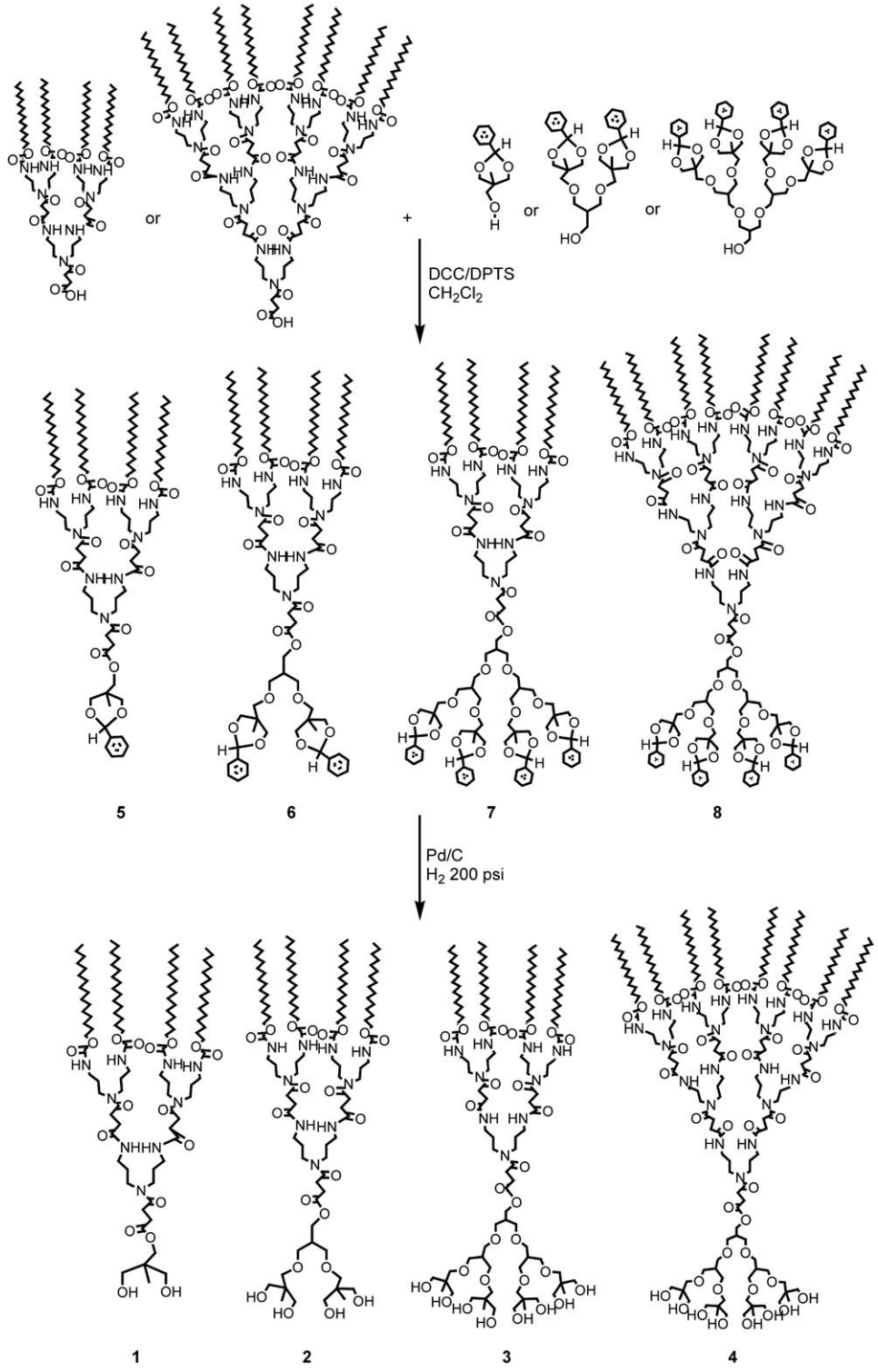


Scheme 1. Schematic structures of diblock codendrimers of PUA and PMDC dendrons with different generations.

eration of the two dendritic blocks independently can adjust their sizes, shapes, and intermolecular interactions. In this way the impact of these factors on self-assemblies can be properly investigated.

## Results and Discussion

**Synthesis and structural features of block codendrimers**: The convergent routes to synthesize dendritic poly(urethane amide) (PUA)[9] and dendritic poly(methallyl dichloride) (PMDC)[10] were employed to generate alkyl-group-modified PUA dendrons and hydroxyl-group-modified PMDC dendrons. The final block codendrimers were obtained by coupling two monodendrons together at the focal groups by using an efficient esterification reaction (Scheme 1).[11] The coupling reaction was followed by catalytic hydrogenolysis to quantitatively remove the benzylidene (Bz) groups to obtain codendrimers with exposed hydroxyl groups at the PMDC moiety. The purity and the structural identity of the codendrimers were assessed by a combination of $^{1}H$ and $^{13}C$ NMR spectroscopies, electrospray ionization time-of-flight (ESI-TOF) and matrix-assisted laser desorption/ionization time-of-flight (MALDI-TOF) mass spectrometries, and elemental analysis (see the Supporting Information).

From compounds **1** to **4**, the chemical structure, molecular architecture, and functional groups are gradually altered by changing the generation of the dendritic blocks. Among compounds **1, 2**, and **3**, the PUA block remains in the second generation and has two amides and four urethanes, whereas the PMDC block increases its generation from the first to the third. Therefore, the number of hydroxyl groups in the periphery of the PMDC block increases from two to eight. Most important is that this increase should augment the polarity, so that these codendrimers are amphiphilic. In compound **4**, the third generation PUA block was coupled with a third generation PMDC block. The clear difference from the other three compounds is the

  

presence of the six amide and eight urethane groups in the PUA block, so the ability of forming inter- or intramolecular hydrogen bonds should be greatly boosted.

**Formation and properties of organic gels**: The codendrimers were found to form transparent gels in toluene or benzene. It is well-known that gel formation is a kinetically controlled process following a nucleation-growth feature.[12] When solutions of the codendrimers in toluene were cooled from 70 °C to an ambient temperature, a limited number of nuclei were created, so a mixture of clear solution with large gel flakes was observed. When the solutions were cooled abruptly by using dry ice/acetone (−78 °C) and then allowed to stand at an ambient temperature, however, the whole solution became immobile and transparent after one day, which indicated the formation of complete gels. This is because rapid cooling creates a great number of nuclei distributing homogeneously through the entire solution. Further growth facilitates the formation of a homogeneous gel.[13] The minimum gel concentrations, $c_{min}$, at which all of the solution became immobile after gelation, are used to describe the gelation ability. From $c_{min}$ we can obtain the value of the number of trapped solvent molecules per codendrimer molecule (TSM/CM). The $c_{min}$ and TSM/CM values of the four codendrimers investigated are listed in Table 1. The results show that the

Table 1. Summary of results from $c_{min}$ measurements, SAXS experiments, and molecular modeling.

| | $M_w$ [g mol$^{-1}$] | $c_{min}$ [g L$^{-1}$] | TSM/CM[a] | Molecular dimension[b] [nm] | Interlamellar spacing[c] [nm] |
|---|---|---|---|---|---|
| **1** | 1834 | 9.6 | 1800 | 4.5 | 9.1 |
| **2** | 2024 | 8.2 | 2320 | 4.9 | 8.5 |
| **3** | 2405 | 7.0 | 3230 | 5.4 | 9.6 |
| **4** | 4331 | 4.2 | 9700 | 6.4 | – |

[a] Number of trapped solvent molecules per codendrimer molecule. [b] Estimated from molecular modeling. [c] Obtained by SAXS experiments on slowly dried gels.

value of $c_{min}$ decreases, whereas TSM/CM increases from codendrimers **1** to **4**, which indicates that the gel-forming ability increases when increasing the generation of the PUA and PMDC blocks. This further illustrates that increasing the polarity by raising the number of hydroxyl groups on the PMDC block and enhancing interactions through the incorporation of more amide groups in the PUA block can improve the gel-forming ability of the codendrimers.

Interestingly, below $c_{min}$ the solution becomes partially immobile and consists of the solvent and gel blocks down to a concentration of 0.1 g L$^{-1}$ (much lower than $c_{min}$ = 7.0 g L$^{-1}$ for compound **3**). Below a concentration of 0.1 g L$^{-1}$, a homogeneous solution is formed. At a concentration of 0.1 g L$^{-1}$, codendrimer **3** can form ribbonlike objects (as shown in Figure 1) like those formed at concentrations above $c_{min}$. This means that over a wide concentration range the codendrimer molecules self-assemble to form aggregates rather than stay molecularly dispersed owing to the multiple

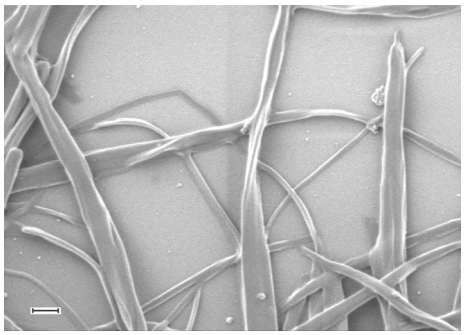

Figure 1. SEM image of the ribbonlike structures found in a solution of **3** in toluene at a concentration of 0.1 g L$^{-1}$. The scale bar is 200 nm.

intermolecular interactions of the dendritic architectures. Therefore, $c_{min}$ means the formation of a complete 3D network of supramolecular structures, rather than mere self-assembly. Interestingly, the solutions of the benzylidene-protected codendrimers did not form gels under the same conditions, which again indicates that the polarities created by the hydroxyl groups in the PMDC periphery are essential for gelation.

**Multiple intermolecular interactions**: FTIR spectra of **3** in the solid state, the gel phase and the sol phase (fresh solution in toluene) are shown in Figure 2 (arrows indicate the peaks studied). It can be seen that the differences between the spectra for the gel phase and solid state are insignificant. However, the bands at $\tilde{\nu}$ = 1721 (C=O stretching), 1524 (N–H bending), 1250 (C–N stretching), and 3330 cm$^{-1}$ (N–H stretching) are shifted to 1686, 1553, 1290, and 3319 cm$^{-1}$, respectively, after gelation from solution, which indicates that upon gelation the amide or urethane groups become

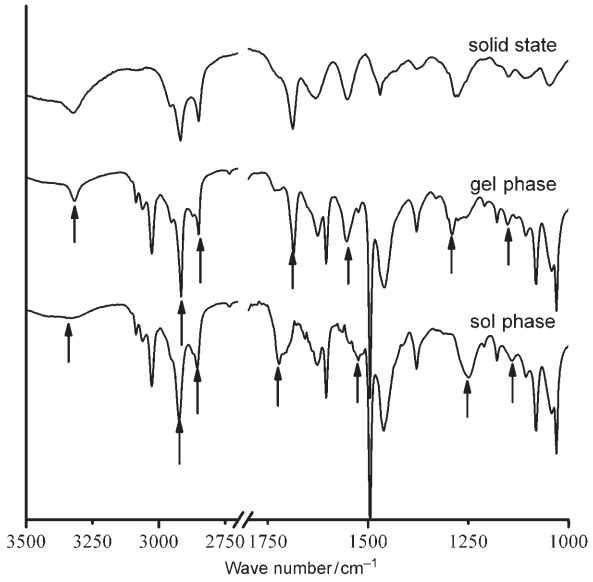


Figure 2. FTIR spectra of **3** in the solid state, the gel-phase and the sol-phase. The solvent is toluene.

strongly hydrogen bonded.[9d,14] Most important to note is that the C–N stretching bands at 1250 (in solution) and 1290 $cm^{-1}$ (in the gel phase) have a *trans* formation of the amide and urethane groups, which indicates the formation of intermolecular hydrogen bonds after gelation. Thus, the IR data clearly indicates that the intermolecular hydrogen bonds between amides and urethanes are a key contribution to gelation.

A broad absorption of the wet gel from 3120 to 3680 $cm^{-1}$ indicates the existence of multiple interactions between the hydroxyl groups on the PMDC blocks, which may be another key factor in assisting gel formation of the codendrimers. We can now understand why the solutions of the benzylidene-protected codendrimers did not form gels under the same conditions: owing to their lack of amphiphilicity, there is no driving force to bring them together. Furthermore, the IR spectra in Figure 2 show that the C–H stretching and rocking bands are shifted from 2924, 2855, and 1139 $cm^{-1}$ to 2916, 2849 and 1151 $cm^{-1}$, respectively, after gelation. This result provides evidence to indicate the formation of a denser packing of the alkyl chains in the gel phase, which is the third factor for assisting gel formation and the stabilization of the supramolecular structure.

As discussed in the previous subsection, the gel-forming ability is improved with increasing the numbers of amide or urethane groups in the PUA blocks and the hydroxyl groups in the PMDC blocks. Our IR studies have provided evidence at the molecular level to verify that the strong interactions, particularly the multiple hydrogen bonds between the PUA blocks in adjacent codendrimers, are the key for forming a stable gel phase. Therefore, it is also understandable that a change in these interactions will affect the gel-forming ability, as indicated in Table 1.

**Supramolecular structures**: It is well-known that gels derived from low molecular mass gelators are supramolecular compounds, which means that the small gelator molecules assemble one- or two-dimensional aggregates at first that further entangle to form self-assembled aggregate networks through a combination of noncovalent interactions.[1] In this work we used transmission electron microscopy (TEM), scanning electron microscopy (SEM), and small-angle X-ray scattering (SAXS) to investigate the self-assembled structures of the codendrimers in the gel phase. The TEM images in Figure 3 show networks of one-dimensional aggregates existing in the gels. The aggregates of compounds **1** and **2** show ribbonlike morphologies that occasionally fuse and intertwine. The aggregates of compounds **3** and **4** show fully cross-linked networks from which we know that the network of **4** is better developed than that of **3**. This is evidence on the nanometer scale to reveal why the gel-forming ability of the codendrimers is improved with increasing the generation of both dendrons. SEM images obtained at a higher magnification in Figure 4 evidently show the ribbonlike aggregates. The ribbon widths are approximately 100 nm for **1**, 80 nm for **2**, 50 nm for **3**, and 30 nm for **4**. This width decrease with the increasing generation further suggests that codendrimers composed of higher-generation dendrons need fewer molecules to construct ribbons with the same ability to build up the three-dimensional network. Unambiguously, this is because increasing the generation of the dendron blocks will result in an increase in the numbers of hydroxyl, amide, and urethane groups in the codendrimers that lead to a higher molecular polarity and stronger interactions. These improvements further promote a highly or-

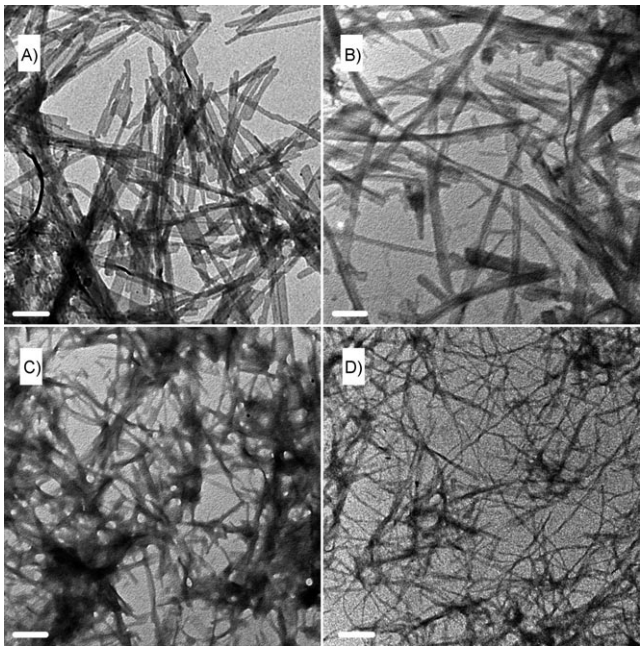


Figure 3. TEM images of dried gels of **1** (A), **2** (B), **3** (C), and **4** (D). The solvent used was toluene and the scale bars are 500 nm.

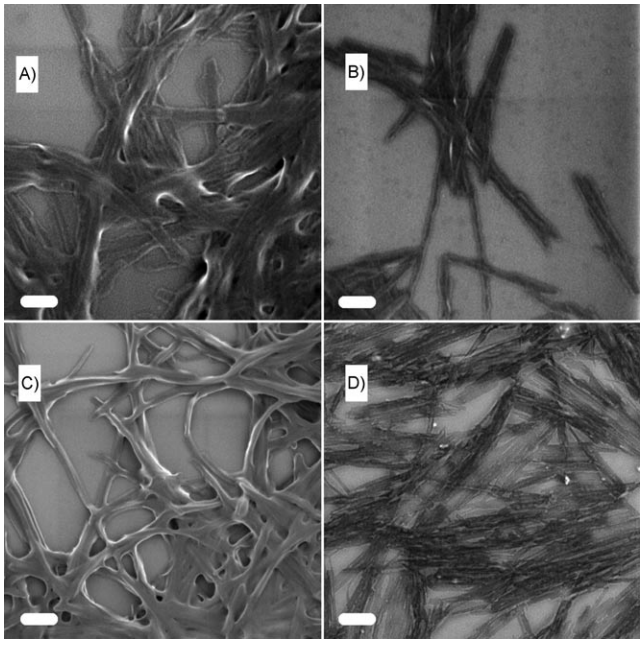


Figure 4. SEM images of dried gels of **1** (A), **2** (B), **3** (C), and **4** (D). The solvent used was toluene and the scale bars are 200 nm.

  

dered arrangement of codendrimers in supramolecular structures. Therefore, the gel-forming ability of codendrimers is enhanced, which exhibits a lowering of the $c_{min}$ on the macroscopic level.

SAXS experiments provide further details of the ribbonlike structures of aggregates **1** to **3** as shown in Figure 5. SAXS patterns of slowly concentrated gels from **1** to **3** showed a lamellar structure with interlayer spacings of 9.1, 8.5, and 9.6 nm, respectively. Considering the molecular dimensions (see Table 1),[15] a layered packing of pairs of molecules can be assumed. For compound **1** the interlayer spacing is twice that of molecular length, which indicates bilayered packing. For compounds **2** and **3**, a dense packing of the segment of the PMDC blocks probably requires an interdigitation of adjacent molecules to avoid free volume.[8a] This is the reason why the interlayer spacing is slightly smaller than twice that of the molecular length of **2** and **3**. To ensure that the slowly concentrated gel maintained the true structure of the wet gel, freeze-drying was used for the gel in benzene. After freeze-drying, the gel remained a cross-linked network of assemblies that had a macroscopically cottonlike appearance. SAXS results of the freeze-dried gel showed almost the same lamellar structure compared to a slowly concentrated gel.

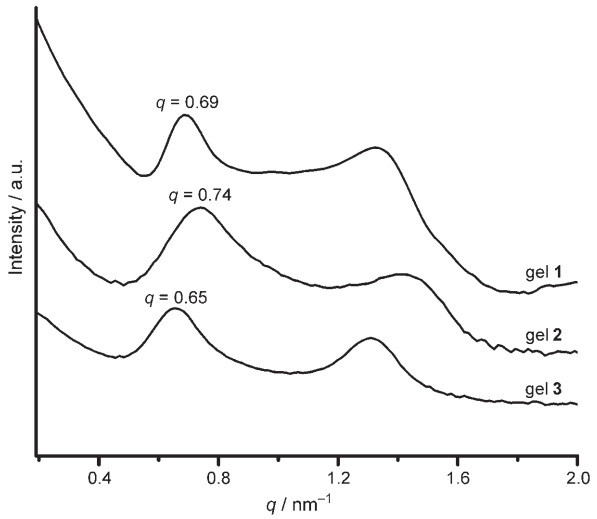


Figure 5. SAXS plots of slowly dried gels of **1** to **3**. The solvent used was toluene.

The scattering peaks in Figure 5 are relatively broad. According to the Scherrer's theory the broad scattering peaks imply only limited numbers of lamellae of compounds **1** to **3** stacked together to form the ribbons.[16] For compound **4**, our scattering study does not show any scattering signals required for structural determination. Possibly, the numbers of the lamellae contained in the ribbons are less than those of the other three codendrimers and may be the reason why **4** shows the best gel-phase forming ability of the four compounds.

**A possible model for ribbon formation**: On the basis of our experimental results, we suggest the simple model shown in Figure 6 to rationalize the formation of ribbonlike structures of the codendrimers. The possible steps are as follows: The hydrogen bonds between hydroxyl groups on the periphery of the PMDC blocks bring the two codendrimers together to form a unit with an interdigitated layer structure. The hydrogen bonds inside the PUA blocks bring the units together to form supramolecules with a ribbonlike structure. During the process, the hydrogen bonds in the *trans* amide and urethane groups result in a face-to-face arrangement between adjacent and fan-shaped PUA blocks. This is the key factor that causes the dominating growth of the ribbons along the direction perpendicular to the PUA face.

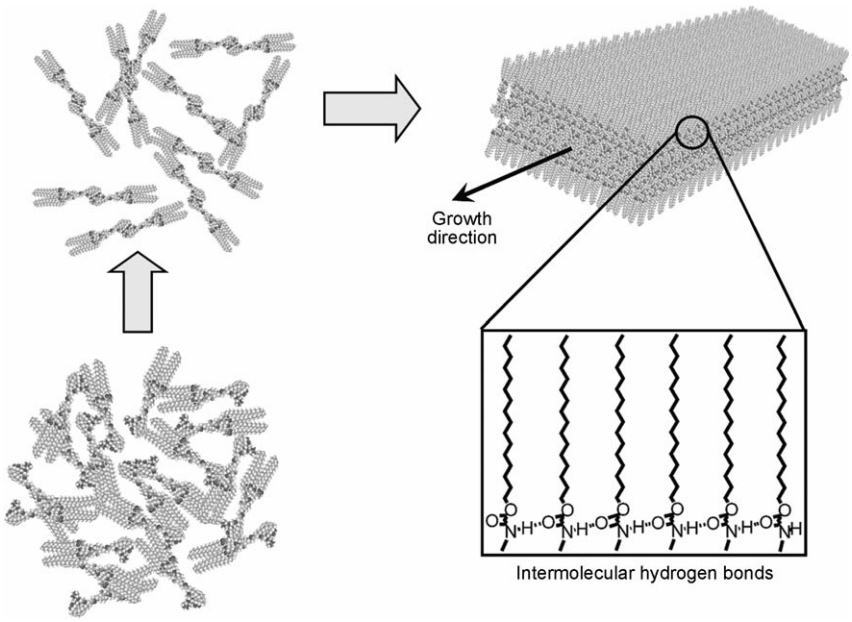


Figure 6. A possible model for ribbon formation of the codendrimers.

## Conclusion

In summary, a series of amphiphilic diblock codendrimers consisting of PUA and PMDC blocks have been synthe-

  

sized. These novel codendrimers were found to self-assemble into ribbonlike aggregates in toluene that could further produce three-dimensional networks behaving macroscopically as gels. Our experimental studies have clearly demonstrated that adjusting the generation of two individual dendrons in the codendrimers can alter the molecular architecture, the polarity ability, and the molecular interactions. One important conclusion is that the high polarity and the multiple molecular interactions, particularly the hydrogen bonds between amide and hydroxyl groups can enhance the gel-forming ability. Our work thus demonstrates that by taking control over molecular parameters of low molecular mass gelators we can control their self-assembly characteristics. Thus, amphiphilic codendritic building blocks provide a new strategy for the rational design of supramolecularly structured functional materials.

## Experimental Section

**Materials**: All reagents and solvents were purchased from major chemical suppliers and used without further purification unless otherwise noted. Dry THF and dry $CH_2Cl_2$ (water content of less than 50 ppm) were purchased from Acros.

**Characterization methods of chemical structures**: The purity and the structural identity of the products were assessed by a combination of TLC, $^1$H and $^{13}$C NMR spectroscopies, ESI-TOF and MALDI-TOF mass spectrometries, and elemental analysis.

TLC was carried out on silica gel coated aluminum plates (0.25 mm silica gel with F254 indicator, MACHEREY-NAGEL, Germany). $^1$H (250 MHz) and $^{13}$C NMR (62.9 MHz) spectra were recorded in $CDCl_3$ or [$D_8$]THF by using a Brucker Spectrospin 250 spectrometer and 700 MHz $^1$H NMR spectra were recorded in $CDCl_3$ by using a Brucker Ultrashield 700 spectrometer. All $\delta$ values are given in ppm relative to tetramethylsilane. MALDI-TOF mass spectrometry was recorded by using a Bruker Reflex II-TOF spectrometer equipped with a 337 nm nitrogen laser. The samples for MALDI-TOF measurements were prepared with a dithranol matrix and potassium salt by using $CH_2Cl_2$ as solvent. Elemental analysis was performed by using an Elemental Vario MICRO CURE instrument.

**Characterization methods of microstructure and properties of gels**: IR spectra were recorded by using a Bio-rad FTS 6000 FT-IR spectrometer with a germanium attenuated total reflectance (ATR) accessory. TEM observations were performed by using a transmission electron microscope (Philips EM420) operated under 120 kV. The samples were prepared by putting the gels on carbon film-coated copper grids. SEM observations were performed by using a LEO 1530 Gemini instrument with an acceleration voltage of 0.5 kV and inlens mode. The gel was transferred to a silica wafer and dried under vacuum before measurements were taken. SAXS experiments were performed by using a Bruker AXS NANOSTAR instrument with a monochromatic X-ray beam and a two-dimensional detector for scattering intensity recording. The distance between the samples and the detector was 1080 mm. The plots of intensity versus the scattering wave vector ($q$), which is calculated from $q=4\pi/\lambda\sin(\theta/2)$ in which $\theta$ is the scattering angle and $\lambda=1.54$ Å for the X-ray beam, were produced by integrating the two-dimensional scattering patterns.

The $c_{min}$ values were measured as follows: The solutions consisting of codendrimer **1** to **4** ($wt_{sample}$: 8, 7, 6, and 3 mg, respectively) and of toluene (1 mL) were prepared as gels. After gelation the lower part of the solution was immobile and the upper part was fluid solvent, which was separated and weighed ($wt_{soln}$). Then $c_{min}$ was calculated by using Equation (1):

$$c_{min}=\frac{wt_{sample}}{1(ml)-\frac{wt_{soln}}{\rho_{toluene}}} \quad (1)$$

The final $c_{min}$ value was an average from three measurements.

**Synthesis of codendrimers C16-PUA-b-PMDC(OH)**

*16g2g1_(OH)$_2$ (**1**)*: Compound (**5**) (112.5 mg, 0.0585 mmol) was dissolved in methanol/$CH_2Cl_2$ (1:1, 20 mL) and Pd/C (10%, 12 mg) was added. The apparatus for catalytic hydrogenolysis was cooled by using liquid $N_2$, the air was evacuated, and it was filled with $H_2$. The reaction was stirred at RT for 5 h. After the reaction was complete, the catalyst was filtered in a glass filter and carefully washed with $CH_2Cl_2$. The filtrate was evaporated to give **1** as a white powder (102 mg, 95%). $^1$H NMR (700 MHz, $CDCl_3$) $\delta=0.88$ (t, $J=7.1$ Hz, 12H; $CH_3$), 1.11 (s, 3H; $CH_3$ (PMDCOH)), 1.25 (s, 104H; $(CH_2)_{13}$), 1.58 (m, 8H; $CH_2CH_2OCO$), 1.66–1.86 (m, 12H; $CH_2CONHCH_2CH_2CH_2NCOCH_2$), 2.54–2.70 (m, 12H; $NCOCH_2CH_2CO$), 3.07–3.37 (m, 24H; $CONHCH_2CH_2CH_2NCO$), 3.57 (s, 4H; $CH_2OH$ (PMDCOH)), 3.98–4.06 (m, 8H; $CH_2CH_2OCO$), 4.17 (s, 2H; $CH_2O$(PMDCOH)), 5.24, 5.32, 5.41, 5.50 ppm (s, 1H; NHCO); $^{13}$C NMR (62.9 MHz, $CDCl_3$): $\delta=14.1$, 17.0, 22.7, 25.9, 27.1, 27.85, 27.92, 28.1, 28.4, 28.9, 29.1, 29.3, 29.6, 29.7, 30.9, 31.0, 31.9, 36.6, 37.0, 37.9, 38.3, 40.7, 45.3, 65.0, 65.1, 67.0, 156.95, 157.00, 157.1, 171.8, 172.5, 172.8, 173.0, 173.9 ppm; MALDI-TOF MS: $m/z$: 1872 $[M+K]^+$; elemental analysis calcd (%) for $C_{103}H_{197}N_9O_{17}$: C 67.46, H 10.83, N 6.87; found: C 67.50, H 10.88, N 6.70.

*16g2g2_(OH)$_4$ (**2**)*: Compound **6** (762 mg, 0.346 mmol) was dissolved in methanol/$CH_2Cl_2$ (1:1, 40 mL) and Pd/C (10%, 76 mg) was added. Compound 16g2g2_$Bz_2$ was deprotected according to the general procedure for the removal of the Bz groups to give **2** as a white powder (690 mg, 98%). $^1$H NMR (700 MHz, $CDCl_3$): $\delta=0.80$ (s, 6H; $CH_3$ (PMDCOH)), 0.88 (t, $J=7.0$ Hz, 12H; $CH_3$), 1.25(s, 104H; $(CH_2)_{13}$), 1.59 (m, 8H, $CH_2CH_2OCO$), 1.64–1.86 (m, 12H; $CH_2CONHCH_2CH_2CH_2NCOCH_2$), 2.23 (m, 1H; $CH_2CHCH_2$ (PMDCOH)), 2.53–2.68 (m, 12H; $NCOCH_2CH_2CO$), 3.06–3.40 (m, 24H; $CONHCH_2CH_2CH_2NCO$), 3.40–3.62 (m, 16H; $OCH_2$ (PMDCOH)), 3.98–4.06 (m, 8H; $CH_2CH_2OCO$), 4.18 (d, $J=5.8$ Hz, 2H; $COOCH2CH$ (PMDCOH)), 5.29, 5.35 5.47, 5.51 ppm (s, 1H; NHCO); $^{13}$C NMR (62.9 MHz, $CDCl_3$): $\delta=14.1$, 17.1, 22.7, 25.8, 27.0, 27.9, 28.5, 29.0, 29.1, 29.58, 29.64, 29.7, 30.88, 30.93, 31.9, 36.8, 37.9, 38.3, 39.3, 41.0, 42.8, 45.3, 50.8, 62.7, 65.0, 65.1, 67.5, 67.6, 75.3, 157.0, 157.1, 171.6, 172.4, 172.7, 172.9, 173.4 ppm; MALDI-TOF MS: $m/z$: 2062 $[M+K]^+$; elemental analysis calcd (%) for $C_{112}H_{215}N_9O_{21}$: C 66.46, H 10.71, N 6.23; found: C 66.44, H 10.65, N 6.32.

*16g2g3_(OH)$_8$ (**3**)*: Compound **7** (529 mg, 0.192 mmol) was dissolved in methanol/$CH_2Cl_2$ (1:1, 30 mL) and Pd/C (10%, 53 mg) was added. 16g2g3_$Bz_4$ was deprotected according to the general procedure for the removal of the Bz groups to give **3** as a white powder (456 mg, 99%). $^1$H NMR (700 MHz, $CDCl_3$): $\delta=0.81$ (s, 12H; $CH_3$ (PMDCOH)), 0.88 (t, $J=7.1$ Hz, 12H; $CH_3$), 1.25(s, 104H; $(CH_2)_{13}$), 1.58 (m, 8H, $CH_2CH_2OCO$), 1.64–1.86 (m, 12H; $CH_2CONHCH_2CH_2CH_2NCOCH_2$), 2.14 (m, 2H; $CH_2CHCH_2$ (PMDCOH)), 2.21 (m, 1H; $CH_2CHCH_2$ (PMDCOH)), 2.52–2.70 (m, 12H; $NCOCH_2CH_2CO$), 3.06–3.40 (m, 24H; $CONHCH_2CH_2CH_2NCO$), 3.40–3.52 (m, 24H; $OCH_2$ (PMDCOH)), 3.56–3.62 (m, $J=10.9$ Hz, 16H; $OCH_2$ (PMDCOH)), 3.98–4.04 (m, 8H; $CH_2CH_2OCO$), 4.10 (d, $J=5.5$ Hz, 2H; $COOCH2CH$ (PMDCOH)), 5.32, 5.40, 5.46, 5.50 ppm (s, 1H; NHCO); $^{13}$C NMR (62.9 MHz, $CDCl_3$): $\delta=14.1$, 17.2, 22.7, 25.9, 28.0, 28.6, 29.1, 29.4, 29.65, 29.69, 30.9, 31.9, 36.8, 38.0, 38.3, 39.2, 40.0, 40.9, 42.9, 45.3, 50.8, 62.9, 65.0, 67.6, 69.1, 69.7, 70.2, 75.9, 157.0, 157.1, 171.7, 172.6, 172.7, 173.0, 173.4 ppm; MALDI-TOF MS: $m/z$: 2442 $[M+K]^+$; elemental analysis calcd (%) for $C_{130}H_{251}N_9O_{29}$: C 64.94, H 10.52, N 6.24; found: C 64.75, H 10.59, N 5.18.

*16g3g3_(OH)$_8$ (**4**)*: Compound **8** (142 mg, 0.0303 mmol) was dissolved in methanol/$CH_2Cl_2$ (1:1, 15 mL) and Pd/C (10%, 15 mg) was added. Compound 16g3g3_$Bz_4$ was deprotected according to the general procedure for the removal of the Bz groups to give **4** as a white powder (127 mg, 97%). $^1$H NMR (700 MHz, $CDCl_3$): $\delta=0.81$ (s, 12H; $CH_3$ (PMDCOH)), 0.88 (t, $J=7.0$ Hz, 24H; $CH_3$), 1.26(s, 208H; $(CH_2)_{13}$), 1.59 (m, 16H; $CH_2CH_2OCO$), 1.72–2.06 (m, 28H; $CH_2CONHCH_2CH_2CH_2NCOCH_2$), 2.14 (m, 2H; $CH_2CHCH_2$ (PMDCOH)), 2.21 (m, 1H; $CH_2CHCH_2$ (PMDCOH)), 2.65 (m, 4H; $COCH_2CH_2CO$(center)), 3.10–3.25 (m, 24H;

  

COC$H_2$C$H_2$CO) 3.30–3.70 (m, 96H; CONHC$H_2$CH$_2$C$H_2$NCO(PUA), OCH$_2$ (PMDCOH)), 4.03 (m, 16H; CH$_2$C$H_2$OCO), 4.14 ppm (d, $J$= 5.6 Hz, 2H; COOC*H*2CH (PMDCOH)); $^{13}$C NMR (62.9 MHz, $CDCl_3$): $\delta$=14.1, 17.2, 22.7, 25.9, 28.0, 29.1, 29.3, 29.6, 29.7, 30.8, 31.9, 36.8, 38.0, 38.4, 40.0, 41.0, 45.4, 65.1, 67.4, 69.1, 69.7, 70.1, 72.9, 75.7, 157.0, 157.1, 172.8, 172.9, 173.1, 173.2 ppm; MALDI-TOF MS: $m/z$: 4369 $[M+K]^+$; elemental analysis calcd (%) for $C_{266}H_{471}N_{21}O_{45}$: C 66.00, H 10.59, N 6.79; found: C 66.12, H 10.56, N 6.87.

*16g2g1_Bz* (***5***): PUA 16g2_COOH (500 mg, 0.289 mmol), PMDC(OH) g1-ol (72 mg, 0.347 mmol, 1.2 equiv), 4-(dimethylamino) pyridinium *p*-toluenesulfonate (DPTS) (85 mg, 0.289 mmol) and dry $CH_2Cl_2$ (10 mL) were mixed in a dry Schlenk tube (25 mL). After the reaction tube was flushed with argon, *N,N'*-dicyclohexylcarbodiimide (DCC) (89.4 mg, 0.434 mmol, 1.5 equiv) was added. The reaction was allowed to stir at RT for 36 h under argon. Once the reaction was complete, the DCC-urethane was filtered off in a glass filter and washed with $CH_2Cl_2$. The crude product was purified by column chromatography on silica gel, eluting with ethyl acetate gradually increasing to 20:80 methanol/ethyl acetate to give **5** as a white powder (478 mg, 86%). $^1$H NMR (700 MHz, $CDCl_3$): $\delta$= 0.82 (s, 3H; CH$_3$ (PMDCOH)), 0.88 (t, $J$=7.1 Hz, 12H; CH$_3$), 1.25 (s, 104H; (CH$_2$)$_{13}$), 1.58 (m, 8H; C$H_2$CH$_2$OCO), 1.64–1.84 (m, 12H; CH$_2$CONHCH$_2$C$H_2$CH$_2$NCOCH$_2$), 2.52–2.72 (m, 12H; NCOC$H_2$C$H_2$CO), 3.07–3.37 (m, 24H; CONHC$H_2$CH$_2$C$H_2$NCO), 3.66 (d, $J$=11.8 Hz, 2H; CH$_2$O (PMDCOH)), 3.98–4.06 (m, 10H; CH$_2$C$H_2$OCO(8H), CH$_2$O(2H; PMDCOH)), 4.40 (s, 2H; CH$_2$O-(PMDCOH)), 5.42 (s, 1H; CHPh), 5.28, 5.30, 5.39,5.46, 6.99, 7.09 (s, 1H; NHCO), 7.34 (m, 3H; Ph), 7.46 ppm (m, 2H; Ph); $^{13}$C NMR (62.9 MHz, $CDCl_3$): $\delta$=14.1, 17.1, 22.7, 25.8, 27.1, 27.6, 27.9, 28.0, 28.5, 28.9, 29.1, 29.4, 29.6, 29.7, 30.9, 31.9, 33.8, 36.7, 37.8, 38.2, 42.5, 45.0, 64.9, 65.1, 66.7, 73.3, 101.9, 126.1, 128.3, 129.0, 138.0, 156.9, 157.1, 171.4, 172.3, 172.5, 172.7, 173.5 ppm; MALDI-TOF MS: $m/z$: 1960 $[M+K]^+$; elemental analysis calcd (%) for $C_{110}H_{201}N_9O_{17}$: C 68.75, H 10.54, N 6.56; found: C 68.80, H 10.43, N 6.61.

*16g2g2_Bz*$_2$ (***6***): PUA 16g2_COOH (800 mg, 0.462 mmol), PMDC(OH) g2-ol (247 mg, 0.508 mmol, 1.1 equiv), DPTS (136 mg, 0.462 mmol), and DCC (143 mg 0.693 mmol) were allowed to react according to the general esterification procedure in dry $CH_2Cl_2$ (10 mL) for 36 h. The crude product was purified by column chromatography on silica gel, eluting with ethyl acetate gradually increasing to 20:80 methanol/ethyl acetate to give **6** as a white powder (961 mg, 95%). $^1$H NMR (700 MHz, $CDCl_3$): $\delta$=0.78 (s, 6H; CH$_3$ (PMDCOH)), 0.88 (t, $J$=7.1 Hz, 12H; CH$_3$), 1.25(s, 104H; (CH$_2$)$_{13}$), 1.58 (m, 8H; C$H_2$CH$_2$OCO), 1.64–1.84 (m, 12H; CH$_2$CONHCH$_2$C$H_2$CH$_2$NCOCH$_2$), 2.29 (m, 1H; CH$_2$C*H*CH$_2$ (PMDCOH)), 2.49–2.68 (m, 12H; NCOC$H_2$C$H_2$CO), 3.04–3.38 (m, 24H; CONHC$H_2$CH$_2$C$H_2$NCO), 3.50–3.60 (m, 8H; OC$H_2$C(CH$_3$)C$H_2$O (PMDCOH)), 3.63 (s, 4H; OC$H_2$C(CH$_3$)C$H_2$O (PMDCOH)), 3.98–4.06 (br d, $J$=11.7 Hz, 12H; CH$_2$C$H_2$OCO(8H), CHC$H_2$O(4H, PMDCOH)), 4.17 (d, $J$=6.1 Hz, 2H; COOC*H*2CH (PMDCOH)), 5.40 (s, 2H; CHPh), 5.26, 5.33 5.48, 5.54, 6.95, 7.04 (s, 1H; NHCO), 7.35 (m, 6H; Ph), 7.46 ppm (m, 4H; Ph); $^{13}$C NMR (62.9 MHz, $CDCl_3$): $\delta$=14.1, 17.5, 22.7, 25.9, 27.1, 27.6, 27.9, 28.0, 28.9, 29.1, 29.3, 29.6, 29.65, 29.69, 31.0, 31.9, 34.6, 36.7, 37.8, 38.3, 39.5, 42.5, 45.0, 63.3, 65.0, 65.1, 69.4, 73.4, 73.5, 101.7, 126.1, 128.2, 128.9, 138.4, 156.9, 157.1, 171.4, 172.3, 172.4, 172.7, 173.4; MALDI-TOF MS: $m/z$: 2223 $[M+Na]^+$, 2239 $[M+K]^+$; elemental analysis calcd (%) for $C_{126}H_{223}N_9O_{21}$: C 68.78, H 10.22, N 5.73; found: C 68.85, H 10.02, N 5.73.

*16g2g3_Bz*$_4$ (***7***): PUA 16g2-COOH (600 mg, 0.347 mmol), PMDC(OH) g3-ol (396 mg, 0.381 mmol, 1.1 equiv), DPTS (102 mg, 0.347 mmol), and DCC (107 mg, 0.521 mmol) were allowed to react according to the general esterification procedure in dry $CH_2Cl_2$ (10 mL) for 36 h. The crude product was purified by column chromatography on silica gel, eluting with ethyl acetate gradually increasing to 20:80 methanol/ethyl acetate to give **7** as a white powder (890 mg, 93%). $^1$H NMR (700 MHz, $CDCl_3$): $\delta$=0.77 (s, 12H; CH$_3$ (PMDCOH)), 0.88 (t, $J$=7.1 Hz, 12H; CH$_3$), 1.25(s, 104H; (CH$_2$)$_{13}$), 1.58 (m, 8H; C$H_2$CH$_2$OCO), 1.62–1.84 (m, 12H; CH$_2$CONHCH$_2$C$H_2$CH$_2$NCOCH$_2$), 2.18 (m, 3H; CH$_2$C*H*CH$_2$ (PMDCOH)), 2.49–2.66 (m, 12H; NCOC$H_2$C$H_2$CO), 3.04–3.37 (m, 24H; CONHC$H_2$CH$_2$C$H_2$NCO), 3.37–3.62 (m, 32H; OC$H_2$C(CH$_3$)C$H_2$O (PMDCOH)), 3.98–4.04 (br d, $J$=11.5 Hz, 16H; CH$_2$C$H_2$OCO(8H), CHC$H_2$O(8H), PMDCOH)), 4.10 (d, $J$=5.9 Hz, 2H; COOC*H*2CH (PMDCOH)), 5.39 (s, 4H; CHPh), 5.27, 5.33, 5.46, 5.50, 6.98, 7.04 (s, 1H; NHCO), 7.34 (m, 12H; Ph), 7.46 ppm (m, 8H; Ph); $^{13}$C NMR (62.9 MHz, $CDCl_3$): $\delta$=14.1, 17.6, 22.7, 25.9, 27.1, 27.6, 27.9, 28.9, 29.08, 29.10, 29.4, 29.65, 29.70, 30.9, 31.9, 34.6, 37.9, 38.3, 39.3, 40.5, 42.6, 45.0, 63.3, 64.9, 65.1, 69.1, 69.8, 73.3, 73.6, 101.7, 126.1, 128.2, 128.8, 138.4, 156.9, 157.0, 171.4, 172.3, 172.4, 172.6, 173.4 ppm; MALDI-TOF MS: $m/z$: 2780 $[M+Na]^+$, 2796 $[M+K]^+$; elemental analysis calcd (%) for $C_{158}H_{267}N_9O_{29}$: C 68.84, H 9.76, N 4.75; found: C 68.70, H 9.84, N 4.73.

*16g3g3_Bz*$_4$ (***8***): PUA 16g3-COOH (300 mg 0.082 mmol), PMDC(OH) g3-ol (103 mg, 0.098 mmol, 1.2 equiv), DPTS (24 mg, 0.082 mmol), and DCC (33.8 mg, 0.164 mmol) were allowed to react according to the general esterification procedure in dry $CH_2Cl_2$ (2 mL) for 24 h (monitored by TLC). The crude product was purified by column chromatography on silica gel, eluting with $CH_2Cl_2$/ethyl acetate/methanol (7/1/1.6) to give **8** as a white powder (352 mg, 92%). $^1$H NMR (700 MHz, $CDCl_3$): $\delta$=0.78 (s, 12H; CH$_3$ (PMDCOH)), 0.88 (t, $J$=7.1 Hz, 24H; CH$_3$), 1.26(s, 208H; (CH$_2$)$_{13}$), 1.59 (m, 16H; C$H_2$CH$_2$OCO), 1.66–1.96 (m, 28H; CH$_2$CONHCH$_2$C$H_2$CH$_2$NCOCH$_2$), 2.18 (m, 3H; CH$_2$C*H*CH$_2$ (PMDCOH)), 2.52–2.80 (m, 28H; COC$H_2$C$H_2$CO), 3.06–3.44 (m, 56H; CONHC$H_2$CH$_2$C$H_2$NCO), 3.44–3.64 (m, 40H; OCH$_2$ (PMDCOH)), 3.98–4.04 (m, 16H; CH$_2$C$H_2$OCO), 4.12 (d, $J$=5.9 Hz, 2H; COOC*H*2CH (PMDCOH)), 5.28 (s, 4H; CHPh), 5.46 (s, 4H; NHCO), 7.34 (m, 12H; Ph), 7.46 ppm (m, 8H; Ph); $^{13}$C NMR (62.9 MHz, $CDCl_3$): $\delta$=14.1, 17.6, 22.7, 25.8, 28.0, 29.1, 29.3, 29.6, 29.7, 30.9, 31.9, 34.5, 36.8, 37.9, 38.3, 40.5, 42.6, 45.1, 63.3, 64.9, 65.1, 69.1, 69.8, 73.3, 73.5, 74.1, 101.7, 126.1, 128.2, 128.8, 138.4, 157.0, 157.1, 171.3, 172.4, 172.5, 172.8, 173.2, 173.4 ppm; MALDI-TOF MS: $m/z$: 4722 $[M+K]^+$; elemental analysis calcd (%) for $C_{266}H_{471}N_{21}O_{45}$: C 68.21, H 10.14, N 6.28; found: C 68.14, H 10.04, N 6.22.

## Acknowledgements

This work was supported by the National Science Foundation of China (NSFC Grant Nos. 20374030 and 20734001). M.Y. thanks the International Max-Planck Research School for supporting his stay in Germany.

[1] a) L. A. Estroff, A. D. Hamilton, *Chem. Rev.* **2004**, *104*, 1201–1217; b) P. Terech, R. G. Weiss, *Chem. Rev.* **1997**, *97*, 3133–3159; c) A. R. Hirst, D. K. Smith in *Low Molecular Mass Gelators: Design, Self-Assembly, Function, Vol. 256*, Springer, Berlin, **2005**, pp. 237–273; d) O. Gronwald, E. Snip, S. Shinkai, *Curr. Opin. Colloid Interface Sci.* **2002**, *7*, 148–156; e) J. H. van Esch, B. L. Feringa, *Angew. Chem.* **2000**, *112*, 2351–2354; *Angew. Chem. Int. Ed.* **2000**, *39*, 2263–2266; f) D. K. Smith, *Chem. Commun.* **2006**, 34–44; g) N. M. Sangeetha, U. Maitra, *Chem. Soc. Rev.* **2005**, *34*, 821–836.

[2] a) F. W. Zeng, S. C. Zimmerman, *Chem. Rev.* **1997**, *97*, 1681–1712; b) D. K. Smith, A. R. Hirst, C. S. Love, J. G. Hardy, S. V. Brignell, B. Q. Huang, *Prog. Polym. Sci.* **2005**, *30*, 220–293; c) T. Emrick, J. M. J. Fréchet, *Curr. Opin. Colloid Interface Sci.* **1999**, *4*, 15–23; d) G. R. Newkome, E. F. He, C. N. Moorefield, *Chem. Rev.*, **1999**, *99*, 1689–1746; e) C. N. Moorefield, G. R. Newkome, *C. R. Chim.* **2003**, *6*, 715–724.

[3] a) V. S. K. Balagurusamy, G. Ungar, V. Percec, G. Johansson, *J. Am. Chem. Soc.* **1997**, *119*, 1539–1555; b) V. Percec, W. D. Cho, P. E. Mosier, G. Ungar, D. J. P. Yeardley, *J. Am. Chem. Soc.* **1998**, *120*, 11061–11070; c) S. D. Hudson, H. T. Jung, V. Percec, W. D. Cho, G. Johansson, G. Ungar, V. S. K. Balagurusamy, *Science* **1997**, *278*, 449–452; d) V. Percec, C. H. Ahn, G. Ungar, D. J. P. Yeardley, M. Moller, S. S. Sheiko, *Nature* **1998**, *391*, 161–164.

[4] a) G. R. Newkome, G. R. Baker, M. J. Saunders, P. S. Russo, V. K. Gupta, Z. Q. Yao, J. E. Miller, K. Bouillion, *J. Chem. Soc. Chem. Commun.* **1986**, 752–753; b) G. R. Newkome, G. R. Baker, S. Arai, M. J. Saunders, P. S. Russo, K. J. Theriot, C. N. Moorefield, L. E. Rogers, J. E. Miller, T. R. Lieux, M. E. Murray, B. Phillips, L. Pascal, *J. Am. Chem. Soc.* **1990**, *112*, 8458–8465; c) G. R. Newkome, C. N.

  

Moorefield, G. R. Baker, R. K. Behera, G. H. Escamillia, M. J. Saunders, *Angew. Chem.* **1992**, *104*, 901–903.

[5] a) K. S. Partridge, D. K. Smith, G. M. Dykes, P. T. McGrail, *Chem. Commun.* **2001**, 319–320; b) B. Q. Huang, A. R. Hirst, D. K. Smith, V. Castelletto, I. W. Hamley, *J. Am. Chem. Soc.* **2005**, *127*, 7130–7139; c) A. R. Hirst, D. K. Smith, M. C. Feiters, H. P. M. Geurts, A. C. Wright, *J. Am. Chem. Soc.* **2003**, *125*, 9010–9011.

[6] a) E. R. Zubarev, M. U. Pralle, E. D. Sone, S. I. Stupp, *J. Am. Chem. Soc.* **2001**, *123*, 4105–4106; b) E. R. Zubarev, E. D. Sone, S. I. Stupp, *Chem. Eur. J.* **2006**, *12*, 7313–7327.

[7] D. K. Smith, *Adv. Mater.* **2006**, *18*, 2773–2778.

[8] a) M. Yang, W. Wang, F. Yuan, X. W. Zhang, J. Y. Li, F. X. Liang, B. L. He, B. Minch, G. Wegner, *J. Am. Chem. Soc.* **2005**, *127*, 15107–15111; b) F. Yuan, W. Wang, M. Yang, X. J. Zhang, J. Y. Li, H. Li, B. L. He, *Macromolecules* **2006**, *39*, 3982–3985; c) F. Yuan, X. J. Zhang, M. Yang, W. Wang, B. Minch, G. Lieser, G. Wegner, *Soft Matter* **2007**, *3*, 1372–1376.

[9] a) S. P. Rannard, N. J. Davis, *Org. Lett.* **2000**, ***2***, 2117–2120; b) S. P. Rannard, N. J. Davis, *Org. Lett.* **1999**, *1*, 933–936; c) M. Llinares, R. Roy, *Chem. Commun.* **1997**, 2119–2120; d) C. Kim, K. T. Kim, Y. Chang, H. H. Song, T. Y. Cho, H. J. Jeon, *J. Am. Chem. Soc.* **2001**, *123*, 5586–5587.

[10] a) M. Jayaraman, J. M. J. Fréchet, *J. Am. Chem. Soc.* **1998**, *120*, 12996–12997; b) S. M. Grayson, J. M. J. Fréchet, *J. Am. Chem. Soc.* **2000**, *122*, 10335–10344.

[11] J. S. Moore, S. I. Stupp, *Macromolecules* **1990**, *23*, 65–70.

[12] R. Y. Wang, X. Y. Liu, J. Y. Xiong, J. L. Li, *J. Phys. Chem. B* **2006**, *110*, 7275–7280.

[13] S. W. Jeong, S. Shinkai, *Nanotechnology* **1997**, *8*, 179–185.

[14] a) W. D. Jang, D. L. Jiang, T. Aida, *J. Am. Chem. Soc.* **2000**, *122*, 3232–3233; b) M. de Loos, J. van Esch, I. Stokroos, R. M. Kellogg, B. L. Feringa, *J. Am. Chem. Soc.* **1997**, *119*, 12675–12676.

[15] Stretched molecular dimensions of the molecules were obtained by using Chem3D with the MM+ force field to give the optimized geometry.

[16] P. Scherrer, *Nachr. Ges. Wiss. Goettingen Math.-Phys. Kl.* **1918**, 2, 96.

Received: November 2, 2007
Published online: February 21, 2008

  